Defense Technical Information Center
Compilation Part Notice

ADP011246

TITLE: Detection of Objects Hidden in Highly Scattering Media Using Time-Gated Imaging Methods

DISTRIBUTION: Approved for public release, distribution unlimited

This paper is part of the following report:

TITLE: Optical Sensing, Imaging and Manipulation for Biological and Biomedical Applications Held in Taipei, Taiwan on 26-27 July 2000. Proceedings

To order the complete compilation report, use: ADA398019

The component part is provided here to allow users access to individually authored sections of proceedings, annals, symposia, etc. However, the component should be considered within the context of the overall compilation report and not as a stand-alone technical report.

The following component part numbers comprise the compilation report:
ADP011212 thru ADP011255

Detection of Objects Hidden in Highly Scattering Media Using Time-Gated Imaging Methods

L. Wang, X. Liang, P. A. Galland, P. P. Ho#, and R. R. Alfano
Institute for Ultrafast Spectroscopy and Lasers
New York State Center for Advanced Technology at CUNY
Departments of Physics and Electrical Engineering
The City College the City University of New York, New York, NY 10031

ABSTRACT

Non-linear ultrafast amplification optical gate has been used to detect back-scattered images of objects hidden in diluted Intralipid solutions.

Key words: amplification gate, time gating, polarized gate, optical Kerr gate

1. INTRODUCTION

To directly detect objects hidden in highly scattering media, the diffusive component of light needs to be sorted out[1-11] from early arrived ballistic and snake photons. In the transmission imaging approach, early light imaging techniques such as optical Kerr gate (OKG), streak camera, second harmonic generation cross-correlation gate, and polarization gate have been employed. The back-scattered early light imaging has one major difference from the transmission approach. In the transmission approach, the earliest photons arrive at the detector always carry the direct information of the hidden object embedded in the turbid medium. However, in the back-scattered approach, the first arrival photons will be directly the back-scattered photons from the host material. The later arriving ballistic back-scattered photons from the hidden object will be mixed with other photons (including ballistic, snake, and diffusive) from the host medium. Additional gating mechanism is needed to separate the light scattered back from host medium surrounding the object. In this paper, a $\chi^{(2)}$ nonlinear optical based gated (NLOG) is applied to acquire time resolved back-scattered images. In comparison to our previous results using an OKG based imaging system, back-scattered imaging using parametric amplification based NLOG has greatly improved the sensitivity and signal to noise ratio of the image.

2. PRINCIPLE

The principle governing the implementation of the NLOG is based on the second order nonlinear optical coefficient $\chi^{(2)}$ from materials such as: KTP (KTiOPO$_4$), BBO, etc. under the phase matching condition. A time-gated amplified signal can be obtained through this NLOG process. Optical parametric amplification gate has previously been used in transmission configuration[12]. The output of the amplified signal, I_s, at frequency ω_s, can be expressed as: $I_1 + I_2 = I_s + I_{residue}$. Where the energy conservation $\omega_2 - \omega_1 = \omega_s$ and the momentum conservation $K_2 - K_1 = K_s$ hold. The amplification factor can be expresses as: $I_s(L) = I_1(0)$ [sinh GL/2]^2 and the gain coefficient, $G = 2 \chi^{(2)} \{I_2(0) [\mu \omega_1 \omega_2]/[\varepsilon n_1 n_2]\}^{0.5}$, where I_1 is the input signal intensity at frequency ω_1, I_2 is the gating pulse intensity at frequency ω_2, $I_{residue}$ is the residue energy from the input I_1 and I_2 after the NLOG, L is the interaction length, and $\chi^{(2)}$ is the second order nonlinearity. The amplification gain of the output at ω_s is attributed from the loss of the intense gating pulse at ω_2. An off-axis type II phase matched NLOG is generally used where the polarization of the amplified signal ω_s is perpendicular to the input. The improvement of the S/N from an NLOG can be estimated using an example from the gain equation of $I_s(L) \sim I_1(0)\exp[GL]$. Given G = 0.5mm^{-1} and L = 10-mm, the output signal gain factor after a NLOG is: $I_s(L=10\text{-mm})/I_1(0) = \exp[10\times0.5] \sim 143$.

Correspondence: E-mail: ho@engr.ccny.cuny.edu; Telephone: 212-650-6808; Fax: 212-650-5530

3. METHOD

The schematic diagram of the back-scattered NLOG imaging system is shown in fig.1. A mode-locked YAG laser system which emitted a 40-ps 1064-nm pulse was used as the illumination beam and its second harmonic at 532-nm was used as the gating pulse in NLOG. A 20-mm long phase-matched cut KTP crystal was used as the $\chi^{(2)}$ gain medium. A pair of crossed polarizers was added into an scattered signal $I_1(t)$ at ω_1 (1064nm) before and after the NLOG crystal. Without the gating pulse ω_2 (532nm), the polarization of the input signal (1064-nm) remained unchanged and the 1064-nm beam would be blocked by the second polarizer (Analyzer). With the gating pulse ω_2 on, a portion of the input scattered profile of ω_1 was selected and amplified within the gating pulse duration. The polarization of the amplified output signal was perpendicular to that of the input signal. In this manner, by synchronizing and gradually delaying the gating pulse $I_2(t)$ at ω_2 relative to the input signal $I_1(t)$, the scattered signal intensity profile as a function of different part of $I_1(t)$ could be selectively sliced and the most of the diffusive part could be rejected simultaneously. The time-sliced output NLOG signal ω_s (1064nm) was amplified and then passed through the analyzer. Following that, a narrow band filter centered at ω_s was used to select the NLOG signal at 1064nm. The sample used in the back-scattered imaging was a positive USAF Resolution Power Test Target (RPTT) immersed in the middle of a 5.5 x 5.5 x 10cm^3 (L x W x H) cell filled with a 2.2% diluted Intralipid solution.
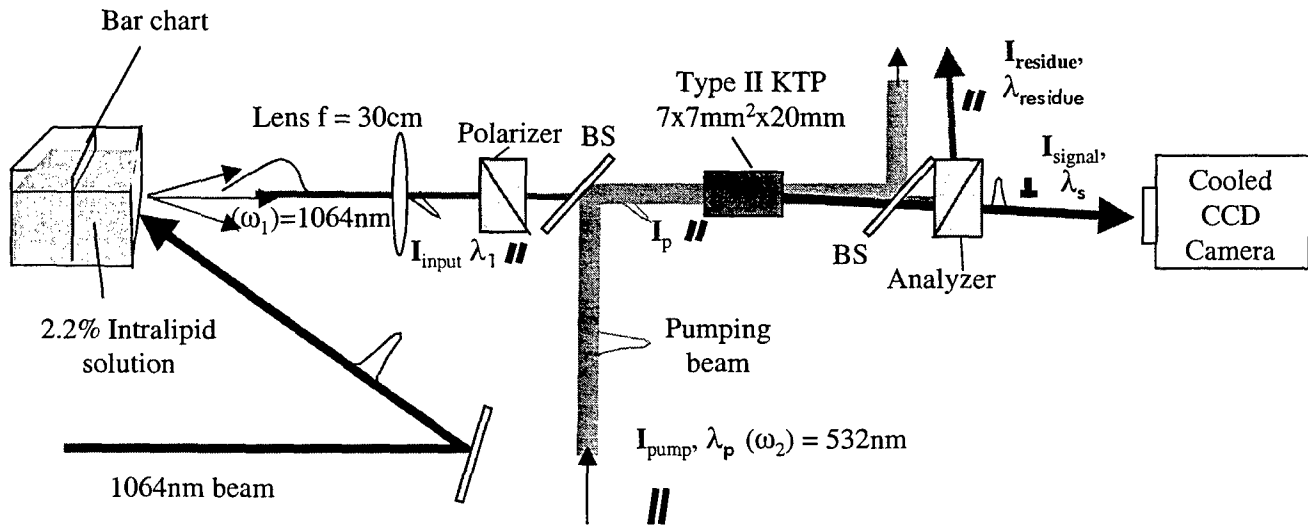

Fig. 1 Experimental setup of a back-scattered imaging system using a $\chi^{(2)}$ NLOG. BS: beam splitter 532 nm reflection /1064 nm transmission. I_{pump}, λ_p = 532nm, pulse width 40ps, pumping beam, frequency 10Hz, power density ~15mJ/(~0.4cm^2) (cross section area at the input of the KTP). I_{signal}, λ_s = 1064nm, amplified input signal component without any background; $I_{residue}$, $\lambda_{residue}$ = 1064nm, signal component with the background present. The amplification factor is ~ 100. Calcite polarizer and analyzer are set perpendicularly and parallel from each other respectively to obtain amplified signal component, I_{signal}, (shown in Fig.2) and amplified residue component $I_{residue}$.

4. RESULTS

Three pictures from the reflection bars of the RPTT under various conditions of the back-scattered imaging from samples using NLOG are displayed in fig. 2. An NLOG image is shown in fig.2a when the RPTT was immersed in a clear water cell. This measurement represents a reference to calibrate the gain factor of the imaging system. By taking the ratio of the images with and without the gating pulse, the absolute gain factor of the NLOG gate was found to be > 100 times at the delay time = 0 and was ~ five times at a time delay of 34-ps. In an image from the RPTT immersed in the diluted Intralipid solution cell was obtained when the gating pulse was off. No image was detected as seen in fig.2b. This picture represented the system minimum background level using a pair of crossed polarizers. An image of RPTT immersed in a 2.2% diluted Intralipid solution was displayed in figure 2c when the gating pulse was on at t = 0 ps. This image signal was greatly amplified and the background noise was low. Beside the improved sensitivity of ~ 100 times, the improved in S/N may also attributed to the change in polarization of the input signal where most of the background was removed.

Using an OKG for a similar back-scattered optical imaging, the reflection test bars can only be imaged through a 3cm long 2% diluted Intralipid solution. The measured image contrast values were ~ 0.80 and 0.65, respectively, in a 5-cm long 2.2% Intralipid

cell using this NLOG and in a 3-cm long 2% Intralipid cell using OKG. The measured scattering length (l_s) of a 2.2% diluted Intralipid solution at 1060-nm was ~ 2.1 mm [ref. 1]. An effective S/N improvement $> 5 \times 10^4 = \exp(-3/0.23) / \exp(-5/0.209)$ was achieved using the NLOG. The larger S/N gain is attributed to the lower background noise from the signal beam.
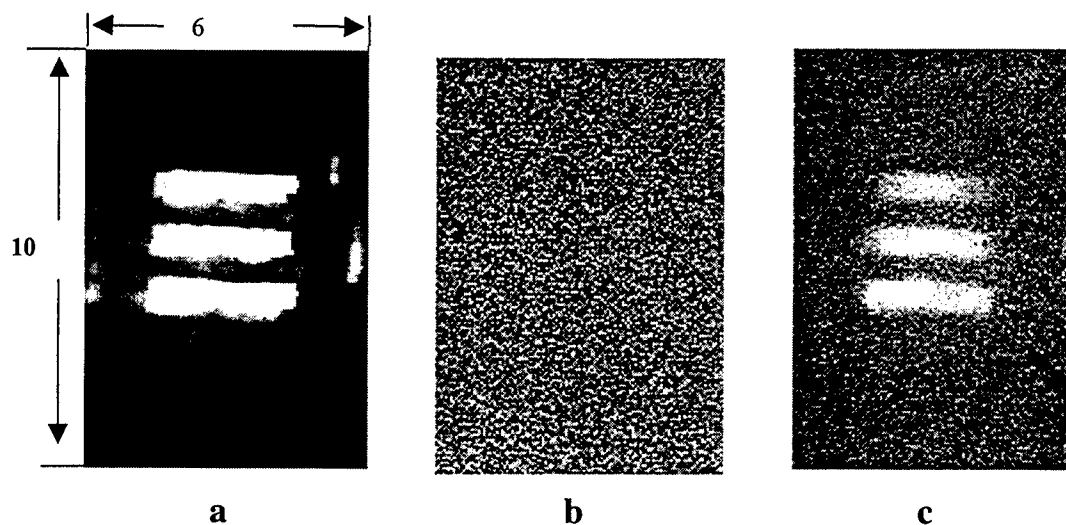

a   b   c

Fig.2. Experimental results from back-scattered from Intralipid using NLOG imaging system. These are images from a section of the reflection bars of an USAF RPTT (1 line pairs/mm) in the middle of a 5.5 x 5.5 x 10 cm^3 plastic cell. The terms: I_s, I_p, $I_{residue}$ are intensity and the subscripts, residue signal, p-pump which provides energy to the input signal; s-signal input signal without the background noise amplified and with a change in polarization from x to y. The measured contrast values are 0.99 and 0.80 for a, and c respectively, and $I_p \perp I_s$
(a) Sample cell filled with clear water
(b) Sample cell filled with 2.2% diluted Intralipid (No gating pulse)
(c) Sample cell filled with 2.2% Intralipid

ACKNOWLEDGEMENT

REFERENCES

1. "True scattering coefficients of turbid media", L. Wang, X. Liang, P. Ho, R. Alfano, Optics Letters, 20 913-5 (1995)
2. "2D Kerr-Fourier imaging of translucent phantoms in thick turbid media", X. Liang, L. Wang, P. Ho, R. Alfano, Applied Optics, 34 3463-7 (1995)
3. "Fourier spatial filter acts as a temporal gate for light propagating through a turbid media", Q. Wang, L. Wang, X. Liang, P. Ho, R. Alfano, Optics Letters, 20 1498-1500 (1995)
4. "Comparison of nonlinear effects of linearly and circularly polarized picosecond pulses propagating in optical fibers", J. Chen, Q. Liu, P. Ho, R. Alfano, Journal of Optical Society of America, B12 (1995)
5. "Time-resolved transillumination for medical diagnosis", S. Anderson-Engels, R. Berg, S. Svanberg, and O. Jarlman, Opt. Lett. 15, 1178-1180 (1990)
6. "Femtosecond transillumination optical coherence tomography", M. Hee, D. Huang, E. Swanson, J. Fujimoto, Opt. Lett., 18 950-952, (1993)
7. "Photon Migration and Imaging in Random Media and Tissues", B. Chance, R. Alfano, ed. SPIE 1888 , 1993.
8. "Ultrahigh speed photography of picosecond light pulses and echoes", M. A. Duguay and A. T. Mattick, Opt. Let., 10, 2162-2170 (1971)
9. "Time-resolved imaging of translucent droplets in highly scattering media", R. Alfano, X. Liang, L. Wang, P. Ho, Science, 264 1913-1915 (1994)
10. "Snake light tomography", P. Ho, L. Wang, X. Liang, P. Galland, L. Kalpaxis, R. R. Alfano Optics and Photonics, pp23-27, Oct. (1193)

11. "Three-dimensional temporal image reconstruction of an object hidden in highly scattering media by time-gated optical tomography", L. Kalpaxis, L. Wang, P. Galland, X. Liang, P. Ho, R. Alfano, Opt. Lett., 18 1691-3 (1993)
12. "Imaging in diffusive media with ultrafast degenerate optical parametric amplification", J. Watson, P. Georges, T. Lepine, B. Alonzi, A. Brun, Opt. Lett., 20 231-3 (1995)